Liang et al. Advances in Bridge Engineering (2023) 4:21
https://doi.org/10.1186/s43251-023-00098-x

Advances in Bridge Engineering

ORIGINAL INNOVATION

Open Access

Damage identification of Chi River bridge based on vehicle excitation and WPEVCR

Zhuoxi Liang[1], Zhihua Xiong[1,2*], Tuotuo Cong[1], Jingxuan Peng[1] and Gengwang Yan[1]

*Correspondence: zh.xiong@nwsuaf.edu.cn

[1] College of Water Resources and Architectural Engineering, Northwest A&F University, Yangling 712100, Shaanxi, China
[2] Institute of Steel Construction, RWTH Aachen University, Aachen, Germany

Abstract

In order to identify damage of Chi River bridge's superstructure, a damage identification indicator is implemented in the field test, which involves the wavelet packet energy analysis with the feature of dynamic response signals caused by vehicle excitation. On the basis of the field test, a series of numeric models with varied service conditions were developed. The wavelet packet analysis method was utilized to decompose the bridge's acceleration signals at both healthy and damaged status, and the values of Wavelet Packet Energy Variance Change Rate (*WPEVCR)* were obtained. Then, according to the acceleration signal data measured from the field test, the damage assessment of the condition of Chi River bridge was performed by means of the obtained *WPEVCR*. The results demonstrate the capability of *WPEVCR* in localizing and quantifying the bridge damage status. Moreover, another damage indicator based on the Hilbert-Huang Transform (HHT) has been also employed to verify the assessment of *WPEVCR*, and both damage identification approaches indicate that the Chi River bridge is in a healthy service condition.

Keywords: Damage identification, Precast bridge, Wavelet packet energy, Vehicle excitation

1 Introduction

Due to various factors such as the defects in the process of construction and the structure's serving environment, the critical parts of the bridge are susceptible to damage caused by cracks, corrosion, deformation, and so on, which probably lead to the destruction of the overall structure. It is not practical to install expensive and technically complex health inspection devices for huge-numbered and widely distributed small-span bridges in remote areas (Sun et al. 2019). Fortunately, considerable resources have been devoted to investigating simple and economical damage identification methods for these structures (Casas and Moughty 2017; Zhang and Yuen 2022).

With the advancement of wavelet analysis theory, structural damage identification methods based on this technique are becoming increasingly popular. Structural health monitoring (SHM) techniques have been widely used in long-span bridges. However, due to limitations of computational ability and data analysis methods, the knowledge of massive SHM data is not well interpreted. Therefore, applications of Big Data (BD) and artificial intelligence (AI) techniques in bridge SHM are developed, respectively (Sun et al. 2020). Taha et al. suggested the use of wavelet multiresolution analysis (WMRA) as a reliable tool for digital signal processing in SHM systems (Taha et al. 2004). Bayissa et al. presented a new damage identification technique based on the statistical moments of the energy density function of the vibration responses in the time-scale (or time–frequency) domain (Bayissa et al. 2008). Ding et al. described the development of a multi-stage scheme for structural damage warning of the Runyang Cable-stayed Bridge using the measured dynamic responses from an online instrumentation system (Ding et al. 2010). Laboratory study shows that the feature vibration can be extracted successfully by reconstructing the wavelet coefficients (Chen and Gao 2011). Lee et al. proposed a continuous relative wavelet entropy–based reference-free damage detection algorithm for truss bridge structures (Lee et al. 2014). The wavelet analysis in one and two dimensions is applied to investigate and assess the movement behavior of a high-speed train railway bridge by applying acceleration measurements (Mohamed et al. 2017). Exploiting the dynamic response of bridge piers induced by vehicle braking excitation, Yang et al. put forward damage indicators over characteristics in acceleration signals and successfully identified the pier's scouring conditions of a specific bridge (Yang et al. 2021). Yu et al. used the ECD method of wavelet packet energy to identify damage in a replaced bridge beam of the Cangzhou Ziya River and investigated the influence of wavelet functions and decomposition levels on the identification performance (Yu et al. 2013). Wang et al. developed the approach of ECD based on wavelet packet energy to locate and identify damages in ancient wooden structures using the Xi'an Bell Tower as an engineering reference (Wang, et al. 2014). Zhu and Sun et al. introduced the WPERSS indicator and verified its accuracy with simply supported beam and cable-stayed bridge models, considering the influence of noise (Zhu and Sun 2015). She et al. adopted WPERSS combined with machine learning algorithms to assess the state of a three-span bridge (She et al. 2023a). For the damage detection of rural old arch bridges, Zhang Yu et al. introduced an optimized random forest (RF) damage identification system by means of a particle swarm (PSO) algorithm and verified the accuracy of this method by simulating a numerical damage model in a noisy environment (Xiong et al. n.d.), and She et al. utilized damage identification methods based on optimized Back Propagation Neural Network (BPNN) to realize damage evaluation of an arch bridge (She et al. 2023b). Noori et al. proposed a modified wavelet packet energy rate index to identify the location and severity of damage in steel bridges and its capability was validated by the result of numerical simulations (Noori et al. 2018). Although numerous researches have been conducted on the intersection between wavelet packet analysis and bridge damage identification, there is a long way to go to massively apply those methods to practical bridge projects due to the difficulty in obtaining the feature parameters involved and the complicated processing procedure. To this end, a simple and easy-to-implement damage identification approach is developed and applied to assess the operating condition of a specific bridge in this research.

Acceleration signals of the bridge's superstructure under vehicle excitation are collected via acceleration sensors in mobile devices, the hidden damage message contained in those signals will be extracted through wavelet packet energy analysis and finally exhibit in the way of *WPEVCR*. This paper takes a prestressed concrete bridge as an example to demonstrate the ability of *WPEVCR* in locating and quantifying structural damage. It also provides a fast, efficient, and cost-effective means of damage detection for a large number of similar projects.

2 Damage indicator

2.1 Theoretical background

The bridge dynamic response signal is related to the structure's intrinsic properties such as stiffness, damping, and mass distribution itself, which can also be regarded as determined by those critical characteristics. Acceleration signals, as a form of the dynamic response of structures, contain structural damage information as well. However, the structure-related damage information is not directly observable from the signal curve, so frequency domain transformation methods are applied to extract the defect features from it. Wavelet packet analysis is a powerful analytical tool that is capable of decomposing the acceleration signals into different frequency bands to obtain the energy values of each band signal and form the characteristic parameter set (Lee and Yamamoto 1994). Damage indicators reflecting structural damage conditions can be obtained by analyzing and processing the energy values in each frequency band. In this paper, the characteristic energy values of healthy structures are compared with those of structures in different damage scenarios, and the *WPEVCR* metric is derived to serve as a damage assessment criterion.

For the acceleration response signal *x(t)*, the total energy E_x under the *j*-layer wavelet packet decomposition is given by the following equation.

$$E_x = \int_{-\infty}^{\infty} x^2(t)dt = \sum_{m=0}^{2^j-1}\sum_{n=0}^{2^j-1}\int_{-\infty}^{+\infty} x_j^m(t)x_j^n(t)dt \tag{1}$$

where $x_j^i(t)$ is the signal in the *i*- th frequency band under the layer of *j*.

Using the orthogonality condition, the total energy of the signal in each frequency band is obtained as follows.

$$E_x = \sum_{i=0}^{2^j-1} E_{x_j^i} = \sum_{i=0}^{2^j-1}\int_{-\infty}^{+\infty}\left[x_j^i(\mathrm{t})\right]^2 dt \tag{2}$$

where $E_{x_j^i}$ is the signal energy in the *i*- th frequency band under the layer of *j*.

When a structure is damaged, the dynamic response signal of its superstructure will fluctuate and the energy of the corresponding frequency band will either increase or decrease after wavelet packet decomposition (Kim and Melhem 2004). According to this principle, the superstructure dynamic response signals corresponding to various structural damage conditions are processed relying on the test bridge. Then, the signal wavelet packet node energy and the characteristic parameters under each frequency band are analyzed and compared. Finally, the energy's variance change rate of the free decay section in the acceleration response signal is proposed as the identification indicator to determine the location of the structural damage.

The signal energy variance of the bridge acceleration response is obtained from Eq. (3).

$$\sigma^2 = 2^{-j}\left[\sum_{i=0}^{2^j-1}\left(E_{a_j^i} - \overline{E}_{a_j}\right)^2\right] \tag{3}$$

where $\overline{E}_{a_j}$ is the mean value of wavelet packet energy of the decomposed spectrum of layer j of the measured signal. The formula for the damage identification indicator is as follows.

$$WPEVCR = \left|\frac{\sigma_d^2 - \sigma_h^2}{\sigma_h^2}\right| \times 100\% = \left|{\sigma_d^2}\middle/{\sigma_h^2} - 1\right| \times 100\% \tag{4}$$

where *WPEVCR* is the change rate of the wavelet packet energy variance of the acceleration response signal *x(t)* at scale *i*. σ_h^2, σ_d^2 are the signal energy variances of the acceleration response signal when the designated structure is in healthy condition and damage condition, respectively.

2.2 Validation of WPEVCR

To validate the damage identification ability of *WPEVCR*, the Finite Element (FE) model of a simply supported beam is established and its structural acceleration signals are collected by conducting explicit dynamic analysis. The validation beam in Fig. 1 is discretized into 16 beam elements at 1-m intervals. The beam's length is 16 m with a rectangular 2×1.5m cross section. The density, modulus of elasticity and the damping ratio for each order of modalities are 2500 kg/m^3, 31.5 GPa and 0.02, respectively. It is assumed that there are 15 accelerometers equally spaced on the model to capture as many structural vibration modes as possible. To yield the history data at each measurement point, the *rand* command in MATLAB is employed to generate random Gaussian white noise with mean 0 and variance 1, as shown in Fig. 2, which acts as an excitation force load on the 15 nodes distributed across the span. The example adopts the reduction of element stiffness to simulate the damaged state of the structure. Additionally, the damage conditions cover single-damage cases and multi-damage cases and the specific damage settings of varied cases are listed in Table 1.

In this paper, the db20 wavelet basis function with a decomposition level of 3 is selected to decompose the free decaying segments of the corresponding element acceleration signals. Therefore, the signal frequency band is uniformly divided into 8 frequency bands. Taking condition D3 as an example, the acceleration signal of sensor 8 for the healthy case and 10% damaged case is displayed in Fig. 3. Obviously, the variation of the beam before and after the damage cannot be seen directly from the acceleration signals. With Eq. (1), the corresponding subspace signal energy can be calculated for each

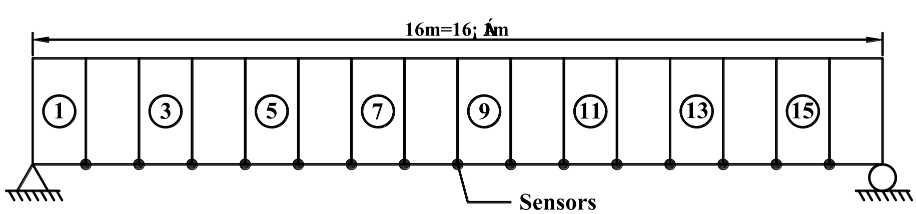

Fig. 1 The layout of the simply supported beam

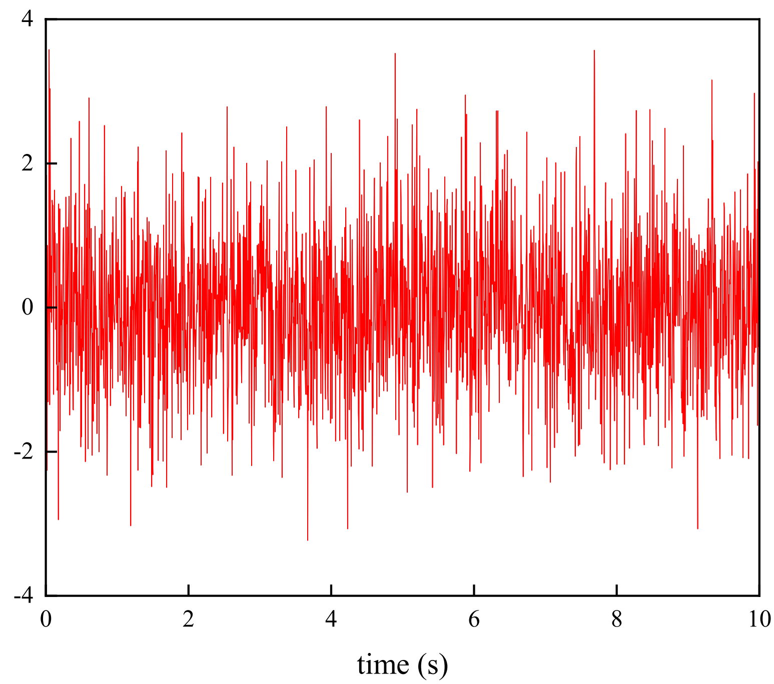

Fig. 2 Gaussian white noise

Table 1 List of damage cases in the simply supported beam

Damage Cases	Number	Damage element	Damage degree
Single damage	D1	Element 2	10%
Single damage	D2	Element 10	10%
Multi-damage	D3	Element 6&13	10%

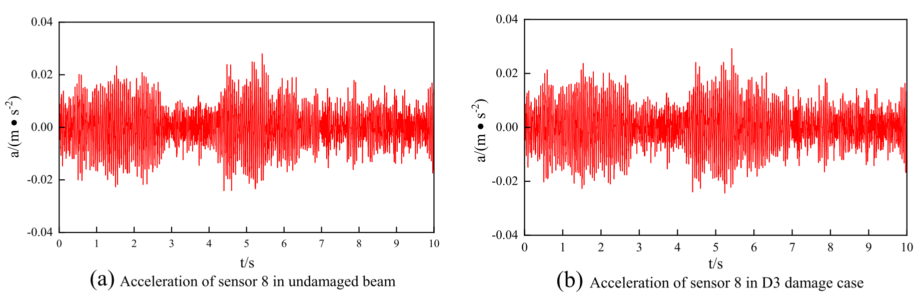

Fig. 3 The acceleration of sensor 8

frequency band composed of the structural signal energy spectrum vector. Finally, the *WPEVCR* value of each measurement point is calculated using Eq. (4).

The wavelet analysis module of MATLAB software realizes the energy feature extraction of the collected acceleration signals. The corresponding *WPEVCR* values of each sensor for three damage cases are calculated by algebraic coding, as shown in Fig. 4. It can be observed that the peak *WPEVCR* appears at the measurement point of the beam

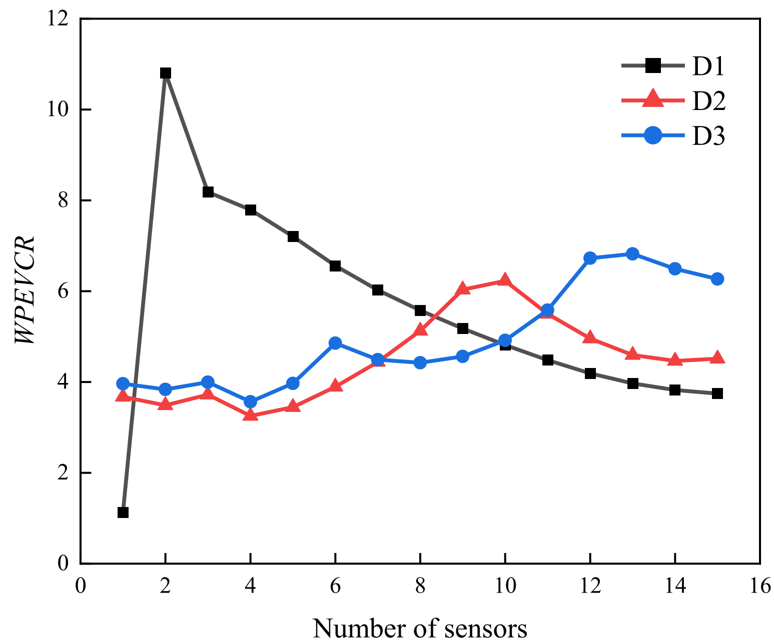

Fig. 4 The *WPEVCR* value of three damage cases

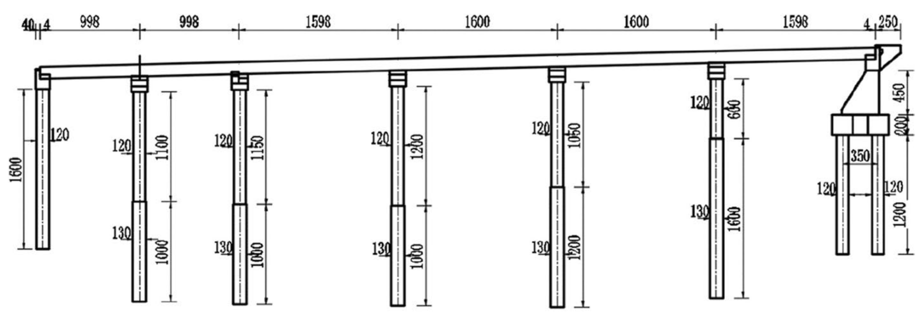

Fig.5 The layout of Chi River bridge

element where the stiffness is compromised in both single-damage and multi-damage conditions. This result suggests that the damage indicator adopted in the paper is capable of accurately locating structural damage and its engineering applicability is as illustrated.

3 WPEVCR of Chi River bridge under various damage status

3.1 Chi River bridge

Chi River bridge crosses the Chi River in Shiquan County, and its total length is 86.94 m with a deck of 7m width as presented in Fig. 5. The bridge consists of a 2×10m cast-in-place reinforced concrete slab approach bridge and a 4×16m precast prestressed concrete slab. The cast-in-place reinforced concrete slabs, cover beams, abutment caps, piers and other bridge components are mainly made of C30 concrete. The aerial view is shown in Fig. 6. In the meantime, the concrete of the prestressed concrete slab, bridge deck and cast-in-place layer is C40. Additionally, the prestressing steel bars are made of

Fig. 6 Aerial view of Chi River bridge

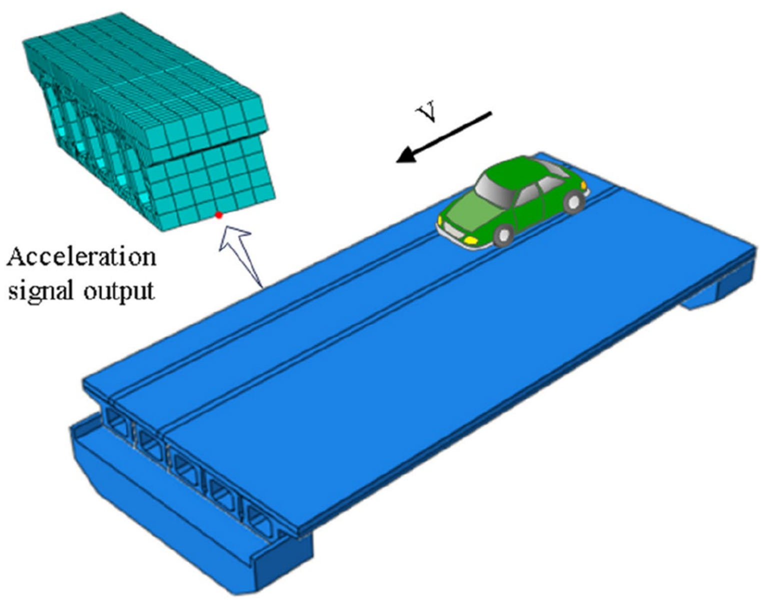

Fig. 7 FE Model

low relaxation stiffness strands with a standard value of tensile strength $f_{pk} = 1860$Mpa, whose nominal diameter d = 15.2mm. Besides, HPB300 and HRB400 reinforcements are used for the common reinforcement in this project.

3.2 Numeric analysis

To accurately simulate the field test process of the main span of this structure, taking the layout of measurement points in field test and bridge type characteristics into consideration, so the finite element software *Abaqus* was adopted to build a span of 16m precast bridge. This model is discretized into 18,468 C3D8R elements with a mesh size of 20cm as shown in Fig. 7, which is in accordance with the practical situation of the bridge. The density and modulus of elasticity of the main girder are 2460 kg/m^3 and 32.5 GPa, respectively.

Sixteen measurement points, 1m between each point, were set up on the FE model in total. The VDLOAD subroutine module is employed to define the position and weight of the front and rear axle, as well as the speed of selected vehicle. Through changing the properties of the damage elements set, the damage reduction of the local structure is achieved, i.e., different damage degrees correspond to various stiffness reduction. Finally, the acceleration response signal at the measurement points is output by performing explicit dynamic analysis on the model.

In the previous study, it is found that even with the same damage level setting, the damage indicators obtained by processing the acceleration response signals at different damage locations can be significantly varied, which indicates that the damage indicators have unique correspondence in particular operating cases. Therefore, the damage situations shown in Table 2 are set up for the FE model of the Chi River bridge to figure out the correlation between the structural damage and the damage identification indicator of this bridge.

With a vehicle speed of 20 km/h, the damage conditions C2, C4, C7, and C8 were executed in the simulation software, and the damage information of 16 points was collected to calculate the *WPEVCR* values, which are plotted in Fig. 8(a, b). It can be observed that the locations of the maximum value of the damage identification indicator in these damage cases coincide with the location of the stiffness discount setting, which means that *WPEVCR* can accurately locate the structural damage.

With the aim of discussing the sensitivity of the damage identification indicator to different damage degrees of Chi River bridge, the single damage of 4 parts and the multi-damage of 4 parts and 13 parts were chosen as examples to set 3 different levels of damage discounting. The *WPEVCR* values were obtained by processing the collected data as displayed in Fig. 8(c, d). From the graphs, it is evident that the peak of the damage identification index still appears at the location of structural damage, while the peak value also tends to become larger with the increase of the damage degree.

3.3 Effects of vehicle axle weight on damage identification index

To demonstrate the efficacy of the damage identification indicator applied in this paper in identifying the location and extent of structural damage regardless of the vehicle axle weight, as well as investigate the effect of vehicle axle weight on the damage identification indicator, the vehicle's weight was changed according to the "Road vehicle outer dimensions, axle load, and mass limits", and the single damage cases were set up in Sect. 4, 8, and 9 as shown in Table 3. After that, finite element analysis is performed keeping the speed of vehicle other variables stable, and *WPEVCR* values are calculated for each measurement point at various damage cases.

Figure 9(a) is the damage identification indicator obtained by setting a vehicle with a single axle weight of 15,500N moves along the bridge when the damage occurred in

Table 2 The damage cases in Chi River bridge

Damage Cases	Number	Damage section	Damage degree
Single damage	C1-C3	Section 4	5%;10%;20%
Single damage	C4-C6	Section 8	5%;10%;20%
Single damage	C7	Section 9	10%
Multi-damage	C8	Section 6&7	10%
Multi-damage	C9-C11	Section 4&13	5%;10%;20%

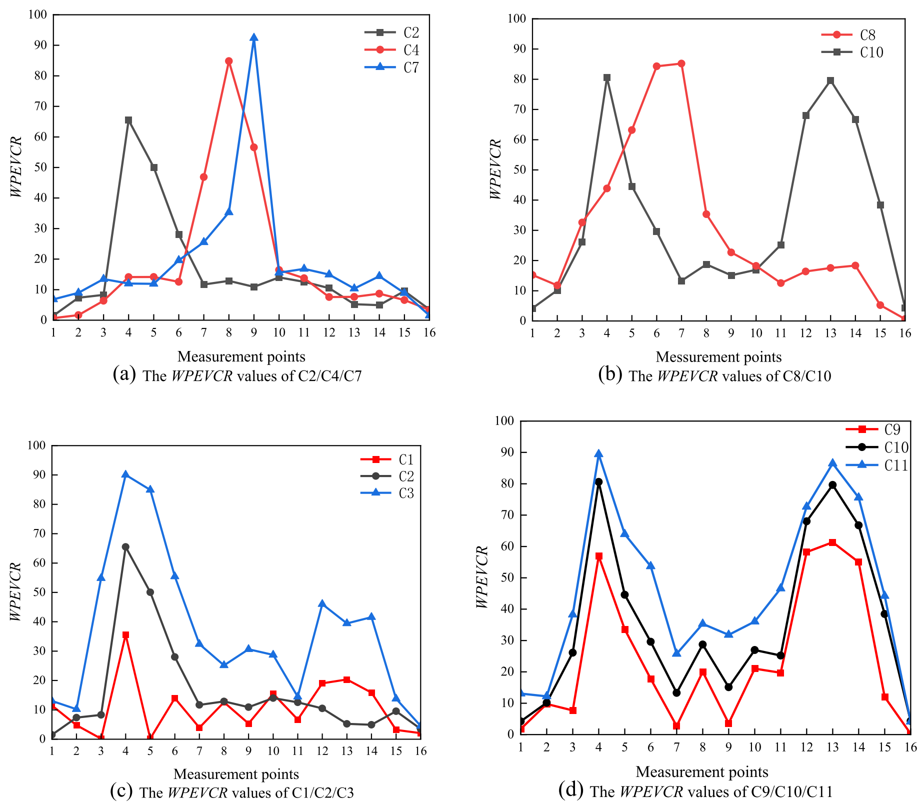

Fig. 8 The *WPEVCR* value of damage cases

Table 3 The damage cases of various axis weight

Damage cases	Single axis weight (N)	Damage section	Damage degree
A_1-A_3	10,500	Section 4	5%;10%;20%
A_4-A_6		Section 8	
A_7-A_9		Section 9	
A_{10}-A_{12}	15,500	Section 4	
A_{13}-A_{15}		Section 8	
A_{16}-A_{18}		Section 9	
A_{19}-A_{21}	20,500	Section 4	
A_{22}-A_{24}		Section 8	
A_{25}-A_{27}		Section 9	

Sect. 8, while Fig. 9(b) is the damage identification indicator obtained by setting a vehicle with a single axle weight of 20,500N moves along the bridge when the damage occurred in Sect. 9. From these figures, it is obvious that the peak value of the damage identification indicators for different axle weight conditions still appears at the same location of the structural damage and the peak value tends to become more significant with the increase of the degree of damage.

Following the data listed in Table 4, altering only the axle weight of the vehicle does not significantly increase or decrease the values of the damage identification indicators obtained with the same settings of damage location and damage degree.

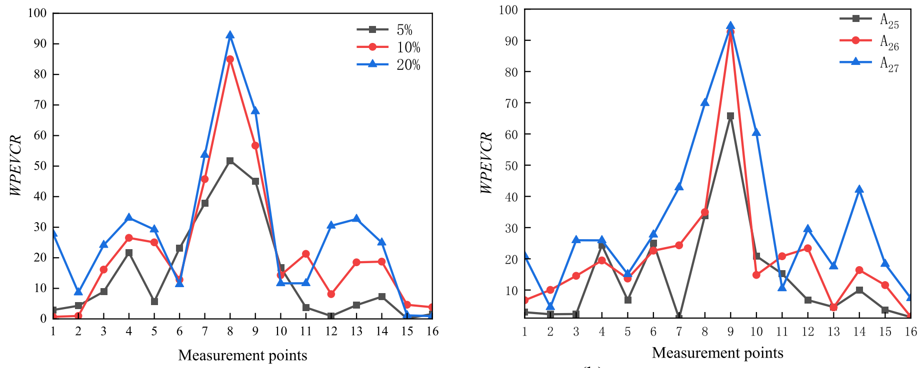

(a) The *WPEVCR* values of $A_{13}/A_{14}/A_{15}$ (b) The *WPEVCR* values of $A_{25}/A_{26}/A_{27}$

Fig. 9 The *WPEVCR* value of damage cases with various axis weight

Table 4 The maximal *WPEVCR* value of various axis weight

Damage cases	*WPEVCR*	Damage cases	*WPEVCR*	Damage cases	*WPEVCR*
A_1	35.61	A_2	65.51	A_3	90.03
A_{10}	36.35	A_{11}	65.83	A_{12}	89.62
A_{19}	35.71	A_{20}	65.44	A_{21}	90.51
A_4	51.62	A_5	84.82	A_6	92.76
A_{13}	51.81	A_{14}	84.99	A_{15}	92.71
A_{22}	51.95	A_{23}	84.53	A_{24}	93.10
A_7	65.41	A_8	92.39	A_9	94.31
A_{16}	67.44	A_{17}	92.45	A_{18}	94.43
A_{25}	65.83	A_{26}	92.63	A_{27}	94.54

However, in the field test, the variation of the damage identification indicator may be more significant due to the self-oscillation noise of different axle-weight vehicles and the interference of environmental noise.

4 Damage assessment of Chi River bridge

4.1 Field test

The field test is conducted to study the self-vibration characteristics of the bridge structure and the joint vibration characteristics of the vehicle and bridge. The dynamic signals collected in the field test is an essential factor to assess the operation condition and load-bearing characteristics of Chi River bridge. Vehicle excitation has been implemented as show in Fig. 10, in which the detail of vehicle includes weighted 36.06 kN with a wheelbase of 3.3 m, a front axle weight of 17.50 kN and a rear axle weight of 18.56 kN. The acceleration signals at each measurement point are recorded using a portable acceleration sensor with a sampling frequency of 100Hz when the vehicle moves at the speed of 20 km/h. Moreover, *MATLAB* is employed to plot the acceleration-time curve of the partial acceleration signal. The layout of measurement points in the field test is given in Table 5.

Fig.10 The picture of the field test

Table 5 The layout of measurement points

Number	Location	Number	Location
M1	Middle of the first span	M4	End of the second span
M2	End of the first span	M5	End of the third span
M3	Middle of the second span	M6	Middle of the fourth span

Table 6 The *WPEVCR* values of the field test

Measurement points	Damage degree			Field test
	5%	10%	20%	
M1	26.20	41.04	55.56	9.99
M2	16.00	29.30	52.57	10.00
M3	26.20	41.04	55.56	9.99
M4	16.00	29.30	52.57	9.99
M5	16.00	29.30	52.57	10.00
M6	26.20	41.04	55.56	9.77

4.2 WPEVCR of the test

In the former subsection, it is learned that the measurement points of the field test are distributed in the middle or at the end of the bridge span. In order to diagnose the real condition of the Chi River bridge, the FE model was used to simulate the different damage states of the corresponding measurement points and calculate their *WPEVCR* values. Meanwhile, the acceleration signals of different measurement points collected from the field test were converted to *WPEVCR* values are listed in Table 6.

A conclusion can be drawn from the above Table that the damage level of each measurement section on the bridge is less than 5%, which means the assessed structure is in a healthy condition.

4.3 HHT damage identification of Chi River bridge

For analyzing nonlinear and unstable data, Huang et al. proposed the Hilbert-Huang Transform (HHT) as a time–frequency signal analysis method combining Empirical Modal Decomposition (EMD) part and Hilbert Transformation part (Feldman 2011). As the core of this algorithm, EMD is able to decompose complex data into a finite number of internal modal functions (IMFs) and then performs a Hilbert transform to obtain the instantaneous frequencies. The original signal is then transformed into a Hilbert spectrum to diagnose structural damage (Huang and Wu 2008).

If HHT is performed on the original signal and its marginal spectrum is calculated. Setting the resulting frequency interval $[\omega_{\min}, \omega_{\max}]$ and dividing the interval into frequency bands $\Delta\omega_i(i = 1, \cdots, n)$. Then the spectral value of energy in each band is $(\omega_i), i = 1, \cdots, n$. The maximum value of n depends on the signal length and the sampling frequency of the signal, the larger the value, the more subdivided the frequency band is.

The definition of the modal component vector is as follows.

$$\xi = \frac{h(\omega_i)}{\sum_{i-1}^{n} h(\omega_i)}(i = 1, 2, \cdots, n) \tag{5}$$

where ξ is the relative proportion of each frequency band component of an IMF signal. The degree of nonlinear deformation of the structural response signal can be represented by numerically processing the change of the modal component vector ξ when the structure is healthy or damaged.

ξ^h, ξ^d are defined as the modal component vectors of the healthy bridge structure and the bridge structure in the real state, respectively, then the damage identification index, the modal vector Euclidean distance, is calculated as below.

$$D = \sqrt{\frac{\sum_{i=0}^{n} \left(\xi^d - \xi^h\right)^2}{n}} \tag{6}$$

The larger the value of the damage indicator corresponds to the greater variation in the frequency band distribution of each mode in the structural response of the bridge, i.e., the more severe the damage is. Conversely, a damage indicator value approaching zero signifies a healthy and undamaged bridge structure.

To ensure the reliability of the damage identification results as well as to validate the damage identification results of *WEPVCR*, *MATLAB* was implemented to code the process of calculating the damage indicator$D$, which is based on the Hilbert-Huang transform. The values of D calculated from the signal outputs of different damage conditions in the FE model and the field tests are listed in Table 7. The results show that the damage

Table 7 The *D* values of the field test

Measurement points	5%	10%	20%	Field test
M1	0.0211	0.0268	0.0276	0.0201
M2	0.0256	0.0285	0.0291	0.0238
M3	0.0211	0.0268	0.0276	0.0207
M4	0.0256	0.0285	0.0291	0.0228
M5	0.0256	0.0285	0.0291	0.0244
M6	0.0211	0.0268	0.0276	0.0203

level of each measurement point of this bridge is less than 5%. In other words, the measured bridge section is in healthy condition and this outcome is similar to the damage identification results based on wavelet packet analysis.

5 Conclusions

- Chi River Bridge is tested and the acceleration signals excited by vehicle load are obtained as the primary information for structural damage analysis. The structural health information of the bridge superstructure is extracted in the form of damage identification indicator *WPEVCR*, which is able to localize the damage accurately by means of maximum value.
- Comparing the damage identification results based on *WPEVCR* and *HHT*, it's obvious that the damage level of the measured superstructure is less than 5% and it's in a healthy service condition. At the same time, the adopted damage identification method based on wavelet packet analysis is effective.
- By altering the axle weight of the vehicle, the values of *WPEVCR* are obtained, which indicates the independent relationship between the damage identification indicator and the axle weight.

Acknowledgements
The authors are grateful for the help of the Transport Bureau of Shi Quan County.

Authors' contributions
Conceptualization, Z. Xiong; Methodology, Z. Xiong and Z. Liang; Investigation, Z. Liang, T. Cong, J. Peng, and G. Yan; Writing—original draft, Z. Liang and T. Cong; Writing—review & editing, Z. Xiong and Z. Liang; Funding acquisition, Z. Xiong; Supervision, Z. Xiong.

Funding
Science and Technology Project of Department of Transport of Shaanxi Province (22-23K).

Availability of data and materials
The datasets used and/or analyzed during the current study are available from the corresponding author upon reasonable request.

Declarations

Competing interests
We declare that we have no known competing financial interests or personal relationships that could have appeared to influence the work reported in this article.

Received: 19 June 2023 Accepted: 16 August 2023
Published online: 07 September 2023

References

Bayissa WL, Haritos N, Thelandersson S (2008) Vibration-based structural damage identification using wavelet transform. Mech Syst Signal Process 22(5):1194–1215

Casas JR, Moughty JJ (2017) Bridge damage detection based on vibration data: past and new developments. Front Built Environ 3:4

Chen X J, Gao Z F (2011) Data processing based on wavelet analysis in structure health monitoring system. J Compt 6(12):2686–2691

Ding YL, Li AQ, Deng Y (2010) Structural damage warning of a long-span cable-stayed bridge using novelty detection technique based on wavelet packet analysis. Adv Struct Eng 13(2):291–298

Feldman M (2011) Hilbert transform in vibration analysis. Mech Syst Signal Process 25(3):735–802

HuangNE, Wu Z (2008) A review on Hilbert-Huang transform: Method and its applications to geophysical studies. Rev Geophysics 46(2)

Kim H, Melhem H (2004) Damage detection of structures by wavelet analysis. Eng Struct 26(3):347–362

Lee SG, Yun GJ, Shang S (2014) Reference-free damage detection for truss bridge structures by continuous relative wavelet entropy method. Struct Health Monitoring 13(3):307–320
Lee DT, Yamamoto A (1994) Wavelet analysis: theory and applications. Hewlett Packard J 45:44–44
Sayed MA, Kaloop MR, Kim E, Kim D (2017) Assessment of acceleration responses of a railway bridge using wavelet analysis. KSCE J Civil Eng 21:1844–1853
Noori M, Wang H, Altabey WA, Silik AI (2018) A modified wavelet energy rate-based damage identification method for steel bridges. Scientia Iranica 25(6: Special Issue Dedicated to Professor Goodarz Ahmadi) 3210–3230
She JC et al (2023a) Damage identification and test of old arch bridge based on wavelet packet analysis [J]. China Highway 03:110–111. https://doi.org/10.13468/j.cnki.chw.2023.03.032. inChinese
She JC, Xiong ZH, Liang ZX, Mou XL, Zhang Y (2023b) Structural health evaluation of arch bridge by field test and optimized BPNN algorithm. Frattura Ed Integrità Strutturale 65:160–177
Sun LM, Shang ZQ, Xia Y (2019) Development and Prospect of Bridge Structural Health Monitoring in the Context of Big Date [J]. China J Highway Transport 32(11):1–20
Sun L, Shang Z, Xia Y, Bhowmick S, Nagarajaiah S (2020) Review of bridge structural health monitoring aided by big data and artificial intelligence: From condition assessment to damage detection. J Struct Eng 146(5):04020073
Taha MR, Noureldin A, Osman A, El-Sheimy N (2004) Introduction to the use of wavelet multiresolution analysis for intelligent structural health monitoring. Canadian J Civil Eng 31(5):719–731
Wang X et al (2014) Damage detection of an ancient wood structure based on wavelet packet energy curvature difference [J]. J Vib Shock 33(07):153–159+186. https://doi.org/10.13465/j.cnki.jvs.2014.07.025
Zhang Y Xiong Z, Liang Z, She J, Ma C (2023) Structural damage identification system suitable for old arch bridge in rural regions: random forest approach. CMES-Comput Model Eng Sci 136(1). https://doi.org/10.32604/cmes.2023.022699
Yang TT, Li Y, Lin XQ (2021) Foundation scour identification method based on vehicle braking excitation and wavelet packet energy analysis for continuous beam bridge [J]. China J Highway Transport 34(04):51–60. (in Chinese)
Yu Z et al (2013) Experimental study on bridge damage identification based on wavelet packet energy curvature difference method [J]. J Vib Shock 32(05):20–25. https://doi.org/10.13465/j.cnki.jvs.2013.05.026. inChinese
Zhang Y, Yuen KV (2022) Review of artificial intelligence-based bridge damage detection. Adv Mechanic Eng 14(9):16878132221122770
Zhu JS, Sun YD (2015) Bridge damage identification index based on wavelet packet energy [J]. J Vib Meas Diagn 35(04):715–721

Publisher's Note

Springer Nature remains neutral with regard to jurisdictional claims in published maps and institutional affiliations.